Separability of Intra- and Intermolecular Vibrational Relaxation Processes in the S_1 State of *trans*-Stilbene

S. L. Schultz, J. Qian, and J. M. Jean*

Department of Chemistry, Washington University, St. Louis, Missouri 63130

Received: August 13, 1996; In Final Form: December 2, 1996[⊗]

Detailed time-resolved measurements of anti-Stokes intensities of several high-frequency modes of electronically excited *trans*-stilbene in hexane and methanol are reported. The most striking changes are observed in the ethylenic band at 1570 cm^{-1}. Nonequilibrium population in the $v = 1$ level of this mode is found to exhibit a biphasic decay, which is interpreted as a rapid energy redistribution followed by a slightly slower process that reflects the transfer of excess energy to the solvent. Comparison of the time-dependent intensity changes of several high-frequency bands with those from a model that assumes instantaneous thermalization of the excited state suggests that internal energy randomization is incomplete on the time scale of solute−solvent thermal equilibration process. No evidence of mode specificity in the energy redistribution process is observed. The results show us to place a value of ∼2 ps on the lifetime of the $v = 1$ level of the ethylenic stretching mode of *trans*-stilbene in both hexane and methanol. Conclusions from this work are discussed in the context of other recent time-resolved Raman measurements of vibrational relaxation in this system in both the gas phase and condensed phase.

I. Introduction

Studies of vibrational relaxation of electronically excited molecules in solution have important implications with regard to mode specificity in ultrafast photochemical reactions as well as for understanding the nature of solute−solvent interactions. For large molecules with dense vibrational manifolds, the canonical view of the relaxation process involves two temporally distinct steps.[1] Energy initially deposited in high-frequency Franck−Condon active "doorway" modes undergoes rapid (subpicosecond) intramolecular vibrational redistribution (IVR), resulting in a thermalized solute molecule that has a vibrational temperature higher than that of the surrounding solvent. The thermal equilibration of this hot molecule with the solvent results from vibrational energy transfer (VET) between low-frequency solute modes and solvent degrees of freedom. The time scale of this latter "cooling" process is found to be on the order of 10−50 ps in most of the systems studied. This sequential relaxation process can be represented in an approximate way by the following simple kinetic scheme:

$$\text{A} \xrightarrow{\text{IVR}} \text{B("hot")} \xrightarrow{\text{VET}} \text{B(ambient)}$$

Here A represents the optically prepared state with a nonthermal distribution of vibrational energy and B a state characterized by a Boltzmann distribution of the total vibrational energy. The validity of this picture relies on a clear separation of time scales for the intra- and intermolecular energy transfer processes. In the absence of such a separation, the loss of energy to the solvent competes with the internal redistribution process with the result that the solute may never achieve a Boltzmann distribution of the excess energy.[2] Evidence that these two steps are temporally distinct in complex systems comes mainly from ultrafast transient absorption and emission studies. For example, Mokhtari et al.[3] observed biexponential emission bandwidth and band position dynamics in dye molecules, which was interpreted as resulting from subpicosecond IVR followed by an order of magnitude slower vibrational cooling process. Similar conclusions were reached by Kaiser and co-workers in their transient absorption studies of organic dye molecules in solution.[1] In contrast, recent work by Sension et al.[4] has shown that IVR in the S_1 state of solution phase *cis*-stilbene is incomplete on the time scale of cis−trans isomerization (∼1 ps). Probing the red edge of ground state absorption band of the nascent trans photoproduct, they find that the IVR time is ∼6 ps.

Despite numerous studies of the kinetics of IVR, relatively little is known about energy flow pathways in complex systems. Theoretical studies of isolated systems have demonstrated the sensitivity of IVR dynamics to details of the potential surface.[5,6] If both high- and low-order anharmonic terms in the potential are comparable in magnitude, then the doorway mode can couple effectively to many modes with the result that the flow of population out of the excited mode is not mode-specific. In such a case, the IVR rate scales with the vibrational state density. Such a picture was used by Zewail, Hochstrasser, and co-workers in their pioneering studies of jet-cooled S_1 *trans*-stilbene and anthracene.[7,8] However, recent steady state work on substituted acetylenes carried out under collisionless conditions has suggested that low (third and/or fourth)-order interactions may dominate the IVR dynamics in these systems.[9] In such a case, the flow of energy out of the initially populated modes may be highly mode-specific with the possibility of energy bottlenecks that effectively prevent complete randomization of the excess energy.

In contrast to the large number of studies that have appeared on IVR in isolated systems, relatively few studies have been carried out that directly probe IVR in the solution phase. Solute−solvent interactions open up new pathways for energy flow that may compete with the pathways operable in the isolated system, depending on the relative magnitudes of intra- and intermolecular interactions. In addition, solvent-induced fluctuations of solute levels lead to increased IVR rates in solution compared to the gas phase. For example, for systems with sparse vibrational manifolds, such as methyl halides, low-frequency solvent motions can compensate for energy mismatches in the system, leading to substantially enhanced IVR rates that show significant solvent dependence.[10] In systems

[⊗] Abstract published in *Advance ACS Abstracts,* January 15, 1997.

S1089-5639(96)02454-1 CCC: $14.00 © 1997 American Chemical Society

with dense manifolds, the extent to which solute−solvent interactions influence the intramolecular redistribution process has not been well-studied.

Picosecond pump−probe resonance Raman scattering has been shown to be a useful mode-specific probe of vibrational relaxation in solution.[11−16] In particular, anti-Stokes scattering probes population in excited vibrational levels of a given mode making it a potentially useful method for gaining further insight into the energy redistribution process.

trans-Stilbene serves as a useful prototypical system for detailed studies of nonequilibrium vibrational dynamics in complex molecules for a number of reasons. The vibrational structure of the S_1 state is well-characterized due primarily to the time-resolved Raman and fluorescence work of Gustafson,[17] Hamaguchi and co-workers,[18] and Chiang and Laane.[19] In addition, a substantial amount of data on IVR in the S_1 state of stilbene under collisionless conditions has been obtained by Zewail, Hochstrasser, and co-workers.[7,8] Comparison of detailed studies of the solution-phase system with these results has the potential for elucidating the effects of solute−solvent interactions on the rates and pathways for energy flow. Finally, the S_0-S_1 and S_1-S_n absorption bands are well-situated spectrally for pump−probe studies that utilize the fundamental and second harmonic of a single dye laser. The use of a single source for the pump and probe beams alleviates timing jitter problems associated with independently tunable sources, which would limit the time resolution to be >5 ps, thus making the early stages of the IVR process experimentally inaccessible.

Recently, our group[12,20] and others[21−23] have carried out detailed picosecond Stokes measurements of vibrational relaxation in the S_1 state of *trans*-stilbene in solution following excitation with varying amounts of excess vibrational energy. The probe beam in these studies was resonant with the strongly allowed S_1-S_n transition. It was found that the ν_7 mode (1570 cm^{-1}; predominantly ethylenic ($C_e{=}C_e$) stretch) blue-shifted and narrowed substantially over the first few tens of picoseconds. Using the ethylenic band position as a probe of VET, we and others found the time constant for this process to be in the 10−12 ps range. While these studies provide useful information on the time it takes the S_1 state to thermally equilibrate with the solvent, they shed little light on the nature of the energy transfer processes involved.

More recently, our group reported the first observation of spontaneous anti-Stokes scattering from high-frequency modes in the S_1 state of *trans*-stilbene.[12] Similar results were recently reported by Hester and co-workers.[23] Such experiments have the potential for elucidating the initial stages of the redistribution process. In our study, we observed substantial intensity changes, particularly in the ethylenic band, during the first 3−4 ps following excitation with 3200 cm^{-1} of excess vibrational energy. Using a simple model based on a Boltzmann distribution of the excess energy, we argued that the spectra at short times reflected the evolution of a nonthermal distribution of the excess energy. Following this 3−4 ps period, we observed no intensity in the ethylenic band. This led us to suggest that the spectral evolution of the ethylenic band seen over tens of picoseconds in the time-resolved Stokes spectra reflected the flow of energy to the solvent from low-frequency modes that anharmonically couple to the ethylenic stretching motion. A somewhat different picture was arrived at by Hester and co-workers. They found that the decay time of the ethylenic anti-Stokes intensity was exponential with a time constant of approximately 10 ps, which is comparable to the time scale of the evolution seen in the Stokes spectra. The similarity of this time scale to that found in the Stokes experiments led this group to suggest that the evolution of the ν_7 band in the Stokes spectra was a direct result of population flow out of this mode. If this is the case, then it implies either that IVR occurs very rapidly leading to a "hot" solute that subsequently cools on the 10 ps time scale or that IVR is slow and represents the rate-determining step in the overall thermal equilibration with the solvent. It should be pointed out, however, that their measurements were carried out with 6 ps pulses. The 8 ps instrument response function was not deconvoluted from their decay data. Thus, the limited temporal resolution of their experiment is insufficient to resolve the early stages of the IVR process.

Considerably better time resolution was achieved by Rulliere and co-workers in their CARS study of S_1 *trans*-stilbene.[24] These workers report intensity changes in several high-frequency modes on the subpicosecond time scale, which were attributed to a combination of IVR and solvation dynamics. The frequency resolution in this study, however, was only ∼100 cm^{-1}, thus obscuring much of the information on the dynamics of individual modes. In addition, the time scale probed was 0−5 ps, which is insufficient to resolve the intra- and intermolecular components of the thermal equilibration process.

The results of these studies raise important questions as to the separability of intra- and intermolecular relaxation processes in complex molecules. In this paper we report the measurement of time-dependent absolute anti-Stokes spectra of the S_1 state of *trans*-stilbene over the range 200−1700 cm^{-1} following excitation with considerably less vibrational energy than used previously. The results of these measurements provide clear evidence of both intra- and intermolecular vibrational energy transfer processes and provide new information on the competition between these two relaxation pathways in this important prototypical system. The remainder of this paper is organized as follows: The next section section briefly describes our method for obtaining absolute anti-Stokes intensity changes. Section III presents results obtained from picosecond anti-Stokes measurements of S_1 *trans*-stilbene focusing primarily on the spectral dynamics observed in the double-bond stretching region. The results provide new insight into the nature of the vibrational relaxation process in complex molecules and allow us to make some qualitative comments regarding energy flow pathways in the S_1 state of stilbene. Summary and conclusions are presented in section IV.

II. Experimental Section

trans-Stilbene was obtained from Aldrich Co. and used without purification. The solvents used in this study were spectral grade hexane and methanol obtained from Fischer. The time-resolved resonance Raman spectrometer has been discussed previously.[20] Briefly, the apparatus consists of a synchronously pumped, mode-locked dye laser (Quantronix) amplified at a repetition rate of 1 kHz in a multistage, multipass arrangement modified from the double confocal cavity design of Becker et al.[25] The amplifier was pumped by the second harmonic (527 nm) of a Q-switched, diode-pumped Nd:YLF laser (Spectra-Physics). The gain dye in all experiments was rhodamine 6G. Rhodamine 640 was used as the amplifier dye. The pump beam was obtained by frequency doubling the amplified output using a 1 mm BBO crystal. The probe beam polarization was maintained at the magic angle (54.7°) relative to the pump beam to avoid any changes in relative intensities due to molecular rotation. The Raman scattered light from the probe beam was collimated and focused into a 0.32 m monochromator equipped with a charge-coupled device (Princeton Instruments). Holographic notch filters (Kaiser Optical) were used to filter the probe beam, allowing us to accurately determine the intensities of anti-Stokes transitions down to ∼200 cm^{-1}.

Time-resolved Raman scattering is both a time and frequency resolution technique; thus, care was taken to ensure that our

dye laser was operating at or very near the transform limit in order to give us the maximum spectral resolution for a given temporal pulse width. The results reported here used pulses of approximately 1 ps in duration with a Gaussian spectral width (fwhm) of approximately 15 cm^{-1}.

Absolute anti-Stokes intensity changes were measured using an external intensity standard. This was accomplished by placing a glass microscope slide in the monochromator near the exit port. A few percent of the dispersed probe beam was picked off and sent to a nearby mirror where it was retroreflected back into the CCD. The position of the mirror was adjusted so that the probe beam appeared on a region of the CCD target where there was no anti-Stokes scattering from the stilbene. Neutral density filters were used to adjust the intensity of the reference signal to be comparable to the intensities of the anti-Stokes transitions, thus avoiding saturation of the detector. The integrated reference signal was used to normalize the anti-Stokes spectra at each delay time, thus correcting for long-term drift in laser power during the course of the measurements. Spectra of the S_1 state were obtained via spectral subtraction (i.e., (pump+probe)−pump−probe+dark) as described previously. Signal averaging times were 1.5 h per spectrum. Comparison of the reference intensities obtained for each spectrum showed that the total probe intensity from one spectrum to the next varied by less than 5% about the average. In principle, this normalization procedure does not correct for long-term fluctuations of the second harmonic of the dye laser, which is used as the pump beam; however, the small values of the normalization factors obtained suggest that the error involved in neglecting fluctuations of the pump intensity is less than ∼10%. The ambient temperature was 295 ± 2 K.

Anti-Stokes intensities were obtained by fitting the observed spectral lines to Voigt line shapes using the Spectra-Calc package (Galactic Industries) and using the integrated intensities of the fitted bands.

III. Results and Discussion

The S_0-S_1 transition in *trans*-stilbene is accompanied by significant displacements in several high- and low-frequency in-plane modes.[26] Thus, in principle, depending on the pump conditions, several quanta of vibrational energy can be deposited in each of these modes. We have carried out detailed measurements of anti-Stokes intensities from *trans*-stilbene in hexane and methanol following excitation into the S_1 state with ∼1600 cm^{-1} of excess energy, which corresponds to one quantum of the strongly Franck−Condon active ethylenic stretching (ν_7) mode. The presence of inhomogeneous broadening resulting from solute−solvent interactions as well as thermal excitation of low-frequency modes, however, precludes mode-specific excitation as is possible in isolated systems prepared under ultracold conditions. Despite the presence of spectral broadening, the pump frequency is such that we can safely rule out pump-induced population in levels higher than $\upsilon = 1$ for modes with frequencies >∼1000 cm^{-1}. Thus, the observation of anti-Stokes scattering from these modes under this excitation condition allows us to probe level-specific population dynamics. The intensity of the $\upsilon = 1 \rightarrow \upsilon = 0$ anti-Stokes transition for a given mode can be written[27]

$$I^{1\rightarrow 0} = P_1|\langle S_1|\mu|S_n\rangle|^2|\sum_e \frac{\langle 1|e\rangle\langle e|0\rangle}{\nu_{e1} - \nu_L + i\Gamma_{e1}}|^2\left(\frac{\Gamma_{10}}{(\nu_{10} - \nu_L + \nu_S)^2 + \Gamma_{10}^2}\right) \quad (1)$$

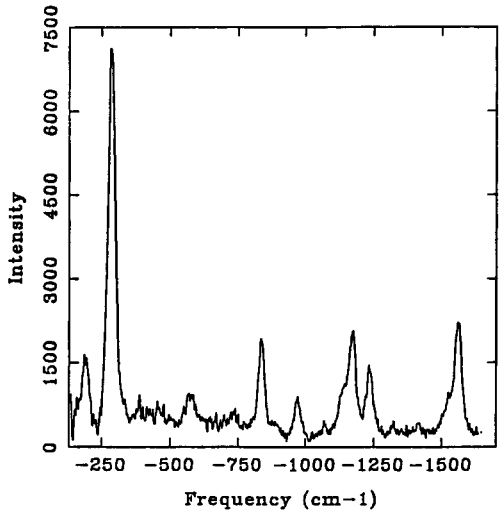

Figure 1. Anti-Stokes spectrum of the S_1 state of *trans*-stilbene in hexane at $t = 0$ ps. Excitation wavelength = 304 nm and probe wavelength = 608 nm.

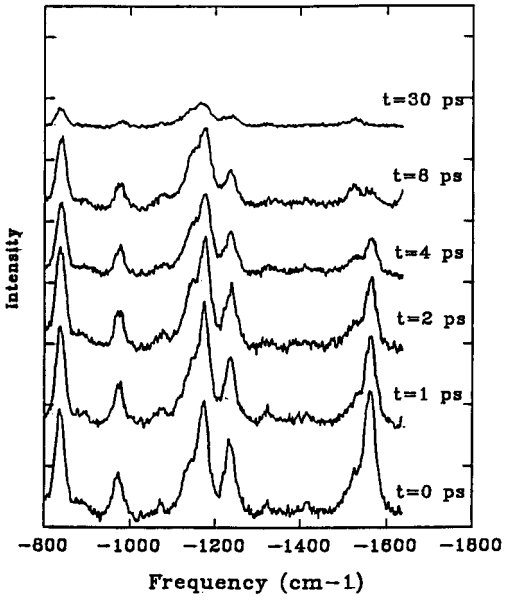

Figure 2. High-frequency anti-Stokes spectra of S_1 *trans*-stilbene in hexane at the indicated delay times.

where P_1 is the population in the $\upsilon = 1$ level and ν_L and ν_S are the probe and scattered frequencies, respectively. $\langle S_1|\mu|S_n\rangle$ is the transition dipole moment for the resonant probe transition, which depends only on the electronic coordinates. Γ_{e1} is the optical dephasing rate of the resonant vibronic transition, and Γ_{01} is the vibrational dephasing rate for the $\upsilon = 1 \rightarrow \upsilon = 0$ transition. The summation runs over all vibrational levels ($|e\rangle$) of the resonant S_n state. Assuming the dephasing rates do not depend strongly on the amount of excess vibrational energy in the molecule, the observed time-dependent intensity of an anti-Stokes transition can be directly related to the $\upsilon = 1$ level population dynamics of the corresponding mode.

The anti-Stokes spectrum of S_1 *trans*-stilbene in hexane obtained at $t = 0$ ps is shown in Figure 1. The most intense band is the 285 cm^{-1} in-plane phenyl ring rocking mode, which is substantially thermally populated at the ambient temperature. In addition, several high-frequency stretching motions also show considerable intensity immediately following the pump process, indicating substantial nonequilibrium population in these modes. Our main goal is to relate the spectral dynamics observed in this region to the underlying energy transfer processes involved in the vibrational relaxation of the S_1 state.

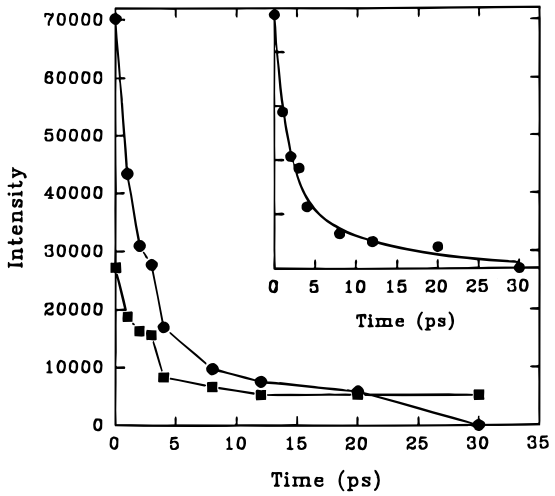

Figure 3. Time-dependent intensities of the ethylenic (●) and phenyl (■) C═C stretching bands. The lines serve to guide the eye. Inset: results of a biexponential fit to the ethylenic intensity, (●) experimental and (—) nonlinear least-squares fit.

Time-resolved spectra of the high-frequency region are shown in Figure 2. Substantial intensity changes are observed for several modes during the first few picoseconds following excitation. The most striking changes are seen in the ethylenic stretching (ν_7) band at 1570 cm^{-1}; thus, we will focus primarily on the dynamics of this mode. The band at 1533 cm^{-1}, which appears as a weak shoulder on the ethylenic band, is assigned to the phenyl C═C stretching motion (ν_8). The C═C region of the spectrum was fit to a sum of two Voigt line shapes allowing the amount of Lorentzian character as well as the bandwidth and position of each to float during the fitting procedure. Figure 3 shows the time-dependent intensities of the two RR-active C═C bands obtained from integrating the fitted spectra. The decay of the ν_7 band is clearly not monoexponential.

In order to gain some insight into the details of the vibrational relaxation process, we discuss this observation in the context of the three-state kinetic model discussed above. This model predicts that the population in an initially excited level will exhibit a biexponential decay. In order to take into account the fact that the S_1 state of stilbene isomerizes, we modify our kinetic scheme to include this parallel process. Here, k_1

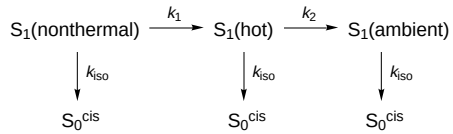

represents the decay of the nonthermal state created by the pump pulse and k_2 represents the slower "cooling" process of the quasi-thermal distribution of the excess energy. k_{iso} is the rate constant for isomerization. A straightforward kinetic analysis gives the following expression for the decay of population in a given mode.

$$P(t) = P_1 e^{-(k_1+k_{iso})t} + P_2 e^{-(k_2+k_{iso})t} + P_a \qquad (2)$$

If $k_1 \gg k_2$ (rapid IVR limit), the amplitudes P_1 and P_2 reflect the initial (nonthermal) and thermalized populations, respectively, of that mode. P_a is the residual population at the ambient temperature.

At this point it is important to point out that we are assuming that only internal pathways exist for the flow of energy out of the high-frequency modes. Direct transfer of one quantum of C═C stretch to the solvent, for example, would require a significant solvent spectral density at ~1600 cm^{-1}. While resonant V—V transfer to localized solvent motions is possible, such a situation would result in a significant dependence of the VET rate on solvent, which is not borne out by our picosecond Stokes studies of S_1 *trans*-stilbene, which show that the VET rate is independent of solvent.[20]

We fit the intensity profile of the ν_7 band to a biexponential decay law assuming the isomerization time (70 ps in hexane at 295 K) is independent of the amount of excess vibrational energy. The inset of Figure 3 shows the actual decay and the biexponential decay, $I(t) = 0.69 \exp(-t/2.4\ \text{ps}) + 0.31 \exp(-t/11.6\ \text{ps})$, obtained from a nonlinear least-squares fit of the experimental data. The short component clearly reflects the flow of nonthermal population out of the $v = 1$ level of the ν_7 mode into lower frequency modes. The majority of the energy is transferred during the first 2—3 ps. The longer component has a time constant (k_2^{-1}) of ~12 ps, which agrees well with the value we and others have obtained for the VET process. The time constant of the fast component allows us to place a lower limit of ~2 ps on the lifetime of the $v = 1$ level of the ν_7 mode.

If intramolecular randomization of the nonthermal population in the ethylenic mode were complete on the 2 ps time scale, then the S_1 state at that point would have a vibrational temperature that is hotter than the ambient solvent. The flow of energy from low-frequency modes into solvent degrees of freedom would be accompanied by rapid redistribution of residual thermal energy from high-frequency modes maintaining a Boltzmann distribution. If this is the case, then the longer component observed in the decay should reflect the time-dependent Boltzmann population of the ethylenic mode. The question then arises as to whether the amplitude of the 12 ps component that we observe is consistent with that expected for the cooling of a thermal distribution.

To answer this question, we compare the longer component of the observed ethylenic intensity decay with the decay predicted from a model in which IVR is assumed to be instantaneous. In this thermal model, we assume the excess energy deposited in the pump process is distributed among the 72 normal modes of the S_1 state at $t = 0$ ps according to Boltzmann. We then calculate the resulting temperature increase using the relation between the temperature and the total vibrational energy, which is given by

$$\langle E_{vib}(T)\rangle = \sum_{i=1}^{3N-6} \left\{ \frac{h\nu_i}{\exp(h\nu_i/kT) - 1} \right\} \qquad (3)$$

where $\langle E_{vib}(T)\rangle = \langle E_{vib}(295\ \text{K})\rangle + E_{excess}$. The temperature is calculated using values for the S_1 frequencies for modes ν_7—ν_{25}, ν_{33}—ν_{37}, ν_{45}—ν_{48}, and ν_{72} obtained from the high-resolution fluorescence excitation work of Urano et al.[18b] For the remaining modes, we use the corresponding frequencies from the infrared and Raman work of Meic and Gusten.[28] The use of ground state frequencies neglects any frequency shifts that occur upon electronic excitation. However, these shifts should be small compared to the values of the actual frequencies and thus not appreciably affect the magnitude of the calculated initial temperature. With this procedure, we find that the vibrational temperature at $t = 0$ is ~385 K. Assuming, as stated earlier, that the vibrational dephasing and optical dephasing rates do not depend on temperature over the range 295—385 K, the anti-Stokes intensity corresponding to the $v = 1$—$v = 0$ transition for any mode i is given by

$$I_i^{1\to 0}(t) = C_i \left\{ \frac{\exp(-h\nu_i/kT(t))}{(1 - \exp(-h\nu_i/kT(t))} \right\} \qquad (4)$$

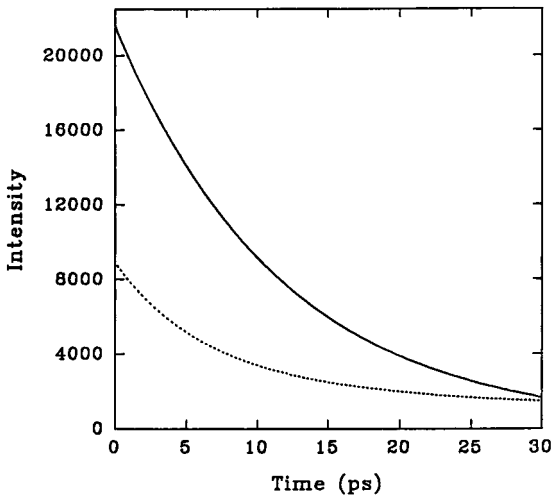

Figure 4. Comparison of the long component obtained from the biexponential fit of the ethylenic band intensity (—) with that obtained from the thermal model.

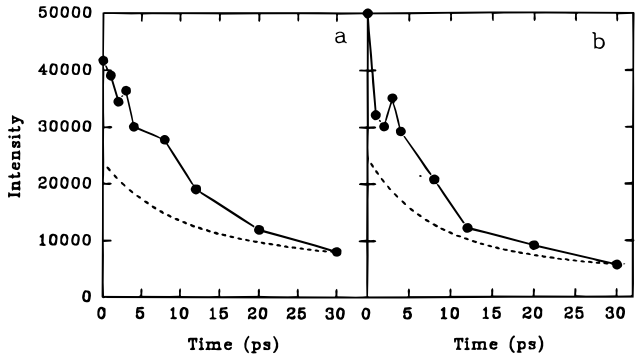

Figure 5. Comparison of experimental anti-Stokes intensity decays (●) with those obtained from the thermal model (- - -): (a) 844 cm^{-1} band and (b) 1236 cm^{-1} band.

where the term in braces is the time-dependent Boltzmann population for the $v = 1$ level. The constant C contains the remaining temperature-independent terms appearing in eq 1. For a given mode, the value of C can be obtained from the observed intensity at $t = 30$ ps, which we take to correspond to the thermally equilibrated (i.e., 295 K) S_1 state. Thus, $C = I(30\ \text{ps})/P_1(295\ \text{K})$. The decay curve for the anti-Stokes intensity can then be determined by assuming the excess energy decays exponentially, i.e., $E_{xs}(t) = E_{xs}(0)\exp(-t/12\ \text{ps})$ and using the relation between thermal energy and vibrational temperature.

Application of this procedure to the ethylenic band is problematic since there is no observable intensity at $t = 30$ ps. In order to obtain a value for the constant C appearing in eq 4, we use the intensity at $t = 30$ ps obtained from the biexponential fit to the data. This value (1450 counts) is probably within the experimental error and can be taken as an approximate upper limit for the ethylenic intensity at 30 ps. A comparison of the decay of the ethylenic band obtained from the thermal model with the long component is shown in Figure 4. As can be seen by the comparison, the amplitude of the longer component is substantially greater than that predicted assuming instantaneous thermalization of the S_1 state. This suggests that the longer component, while reflecting the time scale of energy transfer to the solvent, does not correspond to the "cooling" of a Boltzmann distribution. Thus, the standard picture of rapid and complete IVR leading to a "hot" state, which subsequently cools, does not appear valid in this system.

We have carried out a similar analysis using other high-frequency anti-Stokes bands. Figure 5 shows a comparison of experimental intensities as well as those calculated from the thermal model for the 844 and 1236 cm^{-1} modes. For the 844 cm^{-1} mode we have included the contribution from both the $v = 1$ and $v = 2$ levels. Again, we see that the magnitude of the intensity changes and shapes of the decay curves are not consistent with a rapid intramolecular redistribution process leading to a thermalized solute, which subsequently cools.

At this point it is useful to examine the two main assumptions that go into the thermal model. The first of these is that the optical and vibrational dephasing rates are independent of the solute temperature. Over the range of temperature relevant to this study (295−385 K), this would appear to be reasonable. If the dephasing rates did increase with increasing temperature, as one might expect, then this would have the effect of decreasing the magnitude of the intensity changes during cooling relative to the predictions of our model as can be seen from the form of eq 1. Thus, the thermal model provides an upper limit for the magnitude of the intensity changes expected from the cooling of a Boltzmann distribution. The second assumption is that the matrix elements of the dipole operator are constant throughout the vibrational relaxation process. This would appear to be reasonable so long as there are no substantial conformational changes that accompany vibrational relaxation. Both the S_0 and S_1 states of *trans*-stilbene are known to be planar from studies on the isolated molecule. However, anharmonic effects may lead to changes, for example, in the distribution of the C−phenyl torsional angles as the amount of vibrational energy changes. This would influence the Franck−Condon overlaps between S_1 and S_N vibrational levels, thus affecting the degree of resonance enhancement. If this were the case, then we would expect to see changes in the relative intensities of the various *Stokes* bands during the vibrational relaxation process. Careful measurements of Stokes spectra by us and others clearly show that the relative intensities do not change over the course of relaxation; thus, we conclude that temperature-induced conformational changes are not important in determining the time evolution of the anti-Stokes spectrum.

While these results point out the inseparability of intra- and intermolecular relaxation rates in this system, they provide little insight into internal pathways for energy flow following depopulation of the high-frequency modes. If both low- and higher-order anharmonic interactions play a role in the IVR process, the decay of population initially in high-frequency modes will follow many possible pathways, ultimately resulting in population in low-frequency modes that serve as energy conduits to the solvent. If specific low-order terms dominate the redistribution process, then this may be reflected in the short-time behavior of other modes. For example, it is interesting to compare the dynamics of the ethylenic band with the phenyl C═C band at 1533 cm^{-1}. If strong anharmonic coupling exists between these two modes, we would expect a rapid increase in the population in the ring mode during the first 2−3 ps. The results, however, clearly show that the population of this mode undergoes relatively little change during the IVR process. This suggests that these two motions are isolated from one another on the IVR time scale.

If specific low-frequency motions experience stronger anharmonic coupling to the doorway modes than others, then this should lead to measurable rise times in the intensities of these modes. Careful analysis of the absolute intensity changes in the low-frequency region does not show any evidence for rise times. The lack of observable rise times in the low-frequency region is consistent with a model in which many modes couple to the high-frequency doorway modes. However, one must keep in mind that the RR-active modes comprise only a small fraction of the total vibrational subspace and that the substantial thermal population present in the low-frequency motions may obscure

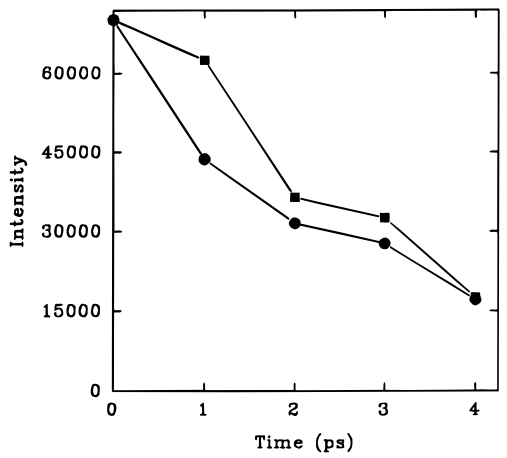

Figure 6. Comparison of the short time ethylenic band intensities in methanol (■) and hexane (●).

any mode-specific dynamics. Studies carried out at substantially reduced ambient temperatures should provide further insight into the pathways for energy flow in this system.

It is interesting to compare the observed value for the time constant of the short component (∼2 ps) with the value of the lifetime of the $v = 1$ level obtained from the $v = 1-v = 0$ line shape. This band is primarily Lorentzian in character as determined by our fitting procedure, suggesting little contribution from broadening mechanisms with time scales slower than that of the Raman process. In the limit of a pure Lorentzian line, the $v = 1-v = 0$ bandwidth (Γ_{10}; fwhm) is related to the vibrational dephasing time (T_2) by $\Gamma_{10} = (\pi T_2)^{-1}$, where $T_2^{-1} = T_1^{-1} + T_2^{*-1}$. The bandwidth for the ethylenic band, obtained after deconvolution of the instrument response, is ∼22 cm^{-1}. Assuming no pure dephasing, we obtain a value of the lifetime of the $v = 1$ level of 480 fs, which represents a lower limit on the IVR time. Using the value of the time constant for the short component of the ethylenic intensity decay, 2 ps, as a measure of the lifetime of the $v = 1$ level, we estimate the pure dephasing time for this mode to be $T_2^* \sim 600$ fs.

We have also carried out anti-Stokes studies of S_1 *trans*-stilbene in methanol. Due to a poorer signal-to-noise ratio than that obtained in hexane, accurate fits of the ethylenic and phenyl C═C bands could only be obtained over the first 4 ps. The reason for the poorer signal quality in methanol may be due to a solvent-induced shift of the S_1-S_n absorption band, thus altering the degree of resonance enhancement of the Raman scattering. In addition, the isomerization rate of *trans*-stilbene in methanol is considerably faster than that in hexane;[29] thus, excited state depletion becomes more problematic. Figure 6 shows a comparison of the time-dependent anti-Stokes intensities of the ethylenic band in methanol and hexane. The data have been scaled to the same initial intensity. The similarity of the decay curves at short times in these two solvents suggests that the initial stages of the intramolecular redistribution process is largely solvent independent. This observation is in sharp contrast to the results obtained on IVR in smaller molecules. As discussed earlier, in systems with vibrationally sparse manifolds, details of the solvent spectral density at low frequencies may have a pronounced influence on the energy redistribution process. In a complex molecule such as stilbene, however, the presence of a number of low-frequency modes results in a continuum of intramolecular states at energies above a few hundred wavenumbers; thus, the rate of the redistribution process is insensitive to details of the solvent spectral density.

Our results show that in the case of the ethylenic mode one can, to some extent, distinguish between IVR and VET. It is thus interesting to discuss our results in the context of the work of Zewail and co-workers on IVR in isolated S_1 *trans*-stilbene.[8,30] Their studies revealed three regimes of IVR, depending on the energy of the initially excited level. Below 750 cm^{-1}, IVR was found to be absent due to insufficient resonant interactions with other degrees of freedom. Between 750 and 1200 cm^{-1}, restricted (coherent) IVR was observed, giving rise to quantum-beat-modulated fluorescence decays. At higher energies, IVR was found to be dissipative with a rate that depends strongly on the amount of excess energy. For example, 25−45 ps components (assigned to IVR) were observed in the decay of fluorescence from the S_1 state following pumping with excess energies in the range 1230−1330 cm^{-1}.[8] In order to extrapolate these results to 1600 cm^{-1}, we assume a golden rule formula for the rate constant,

$$k_{IVR} = (2\pi/\hbar)\langle V^2\rangle\rho(E) \qquad (5)$$

where $\langle V^2\rangle$ is the average anharmonic coupling term and $\rho(E)$ is the vibrational state density. Assuming $\langle V^2\rangle$ is constant over the range 1230−1600 cm^{-1} allows us to predict the IVR rate constant at the excess energy employed in our experiment based on a knowledge of the density of states function. Assuming harmonic modes and using a direct count method, Baskin, et al.[30] report a state density of 570/cm^{-1} at 1280 cm^{-1} and 7900/cm^{-1} at 1830 cm^{-1}. In order to estimate the state density at 1600 cm^{-1}, we assume that log $\rho(E)$ is linear over the relevant range and interpolate, which yields a value of $\rho(1600\ cm^{-1}) \sim 2500/cm^{-1}$. Using eq 5 and the observed IVR time of 35 ps at an excess energy of 1280 cm^{-1}, we estimate the IVR time in the isolated system prepared with 1600 cm^{-1} of excess energy to be ∼8 ps. We note, however, that this value assumes that the average of the square of the anharmonic coupling does not change in going from 1280 to 1600 cm^{-1}. This is a tenuous assumption since excitation at the former energy results in excitation of C−C stretching and C−H bending motions, while excitation at 1600 cm^{-1} populates C═C modes. The magnitude of the anharmonic coupling terms involving single- and double-bond stretching motions may differ considerably.

Zewail and co-workers have also investigated the IVR process in *trans*-stilbene−hexane van der Waals clusters,[31,32] which provides microscopic insight into the role of solute−solvent interactions on the IVR process. The substantial increase in the density of states as a result of the weak coupling to a single hexane solvent molecule was found to have a pronounced effect on the IVR dynamics, lowering the energy of the transition between the coherent and dissipative IVR regimes from 1200 cm^{-1} in the isolated system to 260 cm^{-1}. Thus, while the mechanism of IVR at lower energies is substantially influenced by the increased density of states due to interaction between the solute and a single solvent molecule, the IVR rate at 1600 cm^{-1} in the fully solvated species differs by only a factor of 3 or 4 from that predicted for the isolated system. Further work is required to fully understand the role of solute−solvent interactions on the IVR process in the fully solvated system. One possibility would be to carry out time-resolved anti-Stokes studies as a function of ambient temperature. Such studies would allow one to systematically freeze out solvent fluctuations above a given energy and investigate the effect on the IVR process. At sufficiently low temperatures, the inability of solvent fluctuations to compensate for energy mismatches in the system would lead to bottlenecks in the IVR, which would provide new insight into the nature and magnitude of the important anharmonic interactions in the IVR process.

The results of this work provide a more detailed view of the mechanism of vibrational relaxation of the S_1 state of *trans*-stilbene in solution than that obtained from previous studies. In contrast to Hester and co-workers,[23] we find that the majority

of population in the ethylenic mode is transferred to lower frequency modes on the 2−3 ps time scale. The residual population decays on a time scale that is determined by solute−solvent interactions that lead to the flow of energy out of low-frequency solute modes.

As mentioned in the Introduction, Shkurinov, et al.[24] have recently reported results from pump−probe CARS experiments on the S_1 state of *trans*-stilbene. In their experiments, a subpicosecond pulse populates the S_1 state. Following the pump process, the CARS pulse sequence is applied, and the anti-Stokes spectrum is detected. Their results show spectral evolution of several bands during the first 5 ps. These authors interpret the changes as resulting from conformational changes in the stilbene structure resulting from IVR. The spectral changes observed by these authors occur on a time scale similar to the substantial intensity changes seen in the same spectral region in our experiments. However, we note that whereas in our experiments the spontaneous anti-Stokes scattering from high-frequency modes provides a direct measure of the flow of population initially deposited in the $v = 1$ level by the pump process, the CARS signal receives contribution from population in the ground state ($v = 0$) level of a mode prior to application of the CARS pulse sequence; thus, direct comparison of the results from these two types of experiments does not appear possible.

IV. Summary and Conclusions

Using pump−probe anti-Stokes scattering, we have measured decay times of the population in several low- and high-frequency modes of *trans*-stilbene following excitation into the S_1 state with approximately 1600 cm^{-1} of excess energy. The most striking changes were observed for the ethylenic stretching mode. The decay of population in this mode is clearly nonexponential, reflecting the contribution of intra- and intermolecular energy transfer mechanisms. Comparison of the decay of the ethylenic band with that predicted from a model in which the excess energy is instantaneously randomized among all 72 vibrational modes suggests that IVR is not complete on the time scale of vibrational energy transfer to the solvent. A similar conclusion was reached by examining the decay of several other high-frequency bands. Evidence for extensive but incomplete IVR has also been observed by Fleming and Levy and co-workers[33] in their studies of the excess energy dependence of isomerization rates in *trans*-stilbene and several of its isotopic derivatives performed under isolated conditions.

The picture of the vibrational relaxation process that emerges from this work as well as from our previous time-resolved Stokes studies of S_1 *trans*-stilbene is the following: nonthermal energy initially placed in high-frequency Franck−Condon active modes is largely transferred to lower frequency motions during the first 2−4 ps, leaving only a small "quasi-thermal" population, which decays on a slightly longer time scale. It appears likely that while energy randomization is substantial, the system never completely thermalizes before loss of excess energy to the solvent. Regardless of the extent of energy randomization, the IVR process results in increased excitation of low-frequency modes, which serve to transfer energy to the solvent. This VET process leads to thermal equilibration with the solvent on the 10−12 ps time scale. The loss of excess energy from low-frequency modes that anharmonically couple to the ethylenic stretching motion is responsible for the time-dependent blue shift and band narrowing of the ethylenic band observed in the previous time-resolved Stokes experiments.

Acknowledgment is made to donors of the Petroleum Research Fund, administered by the American Chemical Society, for partial support of this work. We thank Mr. J. J. Zrdrowski for assistance in the analysis of some of the anti-Stokes data and Mr. B. Macgregor for useful discussions.

References and Notes

(1) Elsaesser, T.; Kaiser, W. *Annu. Rev. Phys. Chem.* **1991**, *42*, 83.
(2) Owrutsky, J. C.; Raftery, D.; Hochstrasser, R. M. *Annu. Rev. Phys. Chem.* **1994**, *45*, 519.
(3) Mokhtari, A.; Chesnoy, J.; Laubereau, A. *Chem. Phys. Lett.* **1989**, *155*, 593.
(4) (a) Sension, R. J.; Szarka, A. Z.; Hochstrasser, R. M. *J. Chem. Phys.* **1992**, *97*, 5239. (b) Sension, R. J.; Repinec, S. T.; Hochstrasser, R. M. *J. Chem. Phys.* **1990**, *93*, 9185. (c) Sension, R. J.; Repinec, S. T.; Szarka, A. Z.; Hochstrasser, R. M. *J. Chem. Phys.* **1993**, *98*, 6291.
(5) Sibert, E. L.; Reinhardt, W. P.; Hynes, J. T. *J. Chem. Phys.* **1984**, *81*, 1115.
(6) Stuchebrukhov, A. A.; Marcus, R. A. *J. Chem. Phys.* **1993**, *98*, 6044.
(7) Syage, J. A.; Lambert, Wm.R.; Felker, P. M.; Zewail, A. H.; Hochstrasser, R. M. *Chem. Phys. Lett.* **1982**, *88*, 266.
(8) Felker, P. M.; Zewail, A. H. *Adv. Chem. Phys.* **1988**, *70*, 265. Baskin, J. S.; Felker, P. M.; Zewail, A. H. *Chem. Phys.* **1987**, *86*, 2483.
(9) (a) Gambogi, J. E.; L'Esperance, R. P.; Lehmann, K. K.; Pate, B. H.; Scoles, G. *J. Chem. Phys.* **1993**, *98*, 1112. (b) Lehmann, K. K.; Scoles, G.; Pate, B. H. *Annu. Rev. Phys. Chem.* **1994**, *45*, 241.
(10) Bakker, H. J. *J. Chem. Phys.* **1993**, *98*, 8496.
(11) Hamaguchi, H.; Gustafson, T. L. *Annu. Rev. Phys. Chem.* **1994**, *45*, 593.
(12) Qian, J.; Schultz, S. L.; Jean, J. M. *Chem. Phys. Lett.* **1995**, *233*, 9.
(13) Phillips, D. L.; Rodier, J.-M.; Myers, A. B. *Chem. Phys.* **1993**, *175*, 1.
(14) Weaver, W. L.; Huston, L. A.; Iwata, K.; Gustafson, T. L. *J. Phys. Chem.* **1992**, *96*, 895.
(15) Xu, X.; Lingle, R.; Yu, S.C.; Chang, Y.; Hopkins, J. B. *J. Chem. Phys.* **1990**, *92*, 2106.
(16) Iwata, K.; Yamaguchi, S.; Hamaguchi, H. *Rev. Sci. Instrum.* **1993**, *64*, 2140.
(17) (a) Gustafson, T. L.; Roberts, D. M.; Chernoff, D. A. *J. Chem. Phys.* **1983**, *79*, 1559. (b) Gustafson, T. L.; Roberts, D. M.; Chernoff, D. A. *J. Chem. Phys.* **1984**, *81*, 3438.
(18) (a) Hamaguchi, H.; Urano, T.; Tasumi, M. *Chem. Phys. Lett.* **1984**, *106*, 153. (b) Urano, T.; Hamaguchi, H.; Tasumi, M.; Yamanouchi, S. T.; Tsuchiya, S.; Gustafson, T. L. *J. Chem. Phys.* **1989**, *91*, 3884.
(19) Chiang, W.-Y.; Laane, J. *J. Chem. Phys.* **1994**, *100*, 8755.
(20) Qian, J.; Schultz, S. L.; Bradburn, G. R.; Jean, J. M. *J. Phys. Chem.* **1993**, *97*, 10638.
(21) Iwata, K.; Hamaguchi, H. *Chem. Phys. Lett.* **1993**, *196*, 462.
(22) Hester, R.; Matousek, P.; Moore, J. N.; Parker, A. W.; Toner, W. T.; Towrie, M. *Chem.* Phys. *Lett.* **1993**, *208*, 471.
(23) Matousek, P.; Parker, A. W.; Toner, W. T.; Towrie, M.; de Faria, D. L. A.; Hester, R. E.; Moore, J. N. *Chem. Phys. Lett.* **1995**, *237*, 373.
(24) Schkurinov, A. P.; Koroteev, N. I.; Jonusauskas, G.; Rulliere, C. *Chem. Phys. Lett.* **1994**, *223*, 573.
(25) Becker, P. C.; Prosser, A. G.; Jedju, T.; Kafka, J. D.; Baer, T. *Opt. Lett.* **1991**, *16*, 1847.
(26) Myers, A. B.; Mathies, R. A. *J. Chem. Phys.* **1984**, *81*, 1552.
(27) Ziegler, L. *Acc. Chem. Res.* **1994**, *27*, 1.
(28) Meic, Z.; Gusten, H. *Spectrochim. Acta, Part A* **1978**, *34*, 101.
(29) Kim, K. K.; Courtney, S. H.; Fleming, G. R. *Chem. Phys. Lett.* **1989**, *159*, 543.
(30) Baskin, J. S.; Banares, L.; Pedersen, S.; Zewail, A. H. *J. Phys. Chem.* **1996**, *100*, 11920.
(31) Lienau, C.; Heikal, A. A.; Zewail, A. H. *Chem. Phys.* **1993**, *175*, 171.
(32) Heikal, A. A.; Chong, S. H.; Baskin, J. S.; Zewail, A. H. *Chem. Phys. Lett.* **1995**, *242*, 380.
(33) Courtney, S. H.; Balk, M. W.; Philips, L. A.; Webb, S. P.; Yang, D.; Levy, D. H.; Fleming, G. R. *J. Chem. Phys.* **1988**, *89*, 6697.